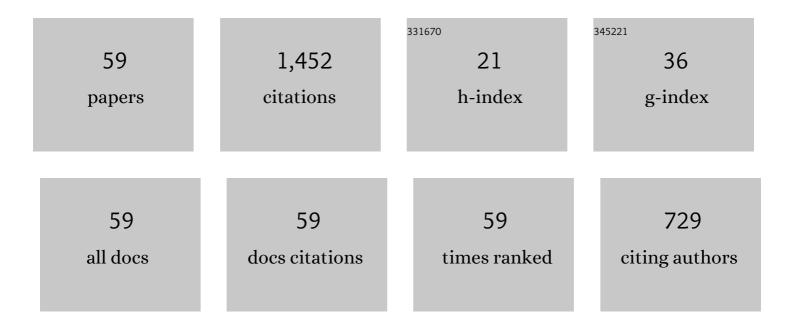
å>¹/2Ç^{|1} ä³/4

List of Publications by Year in descending order

Source: https://exaly.com/author-pdf/866832/publications.pdf Version: 2024-02-01



<u>1/2011 x3/2-</u>

#	Article	IF	CITATIONS
1	Self-grown oxygen vacancies-rich CeO2/BiOBr Z-scheme heterojunction decorated with rGO as charge transfer channel for enhanced photocatalytic oxidation of elemental mercury. Journal of Colloid and Interface Science, 2021, 587, 402-416.	9.4	120
2	Influence of BiOIO3 morphology on the photocatalytic efficiency of Z-scheme BiOIO3/g-C3N4 heterojunctioned composite for Hg0 removal. Journal of Colloid and Interface Science, 2020, 558, 123-136.	9.4	89
3	Bismuth-based photocatalyst for photocatalytic oxidation of flue gas mercury removal: A review. Journal of Hazardous Materials, 2021, 418, 126280.	12.4	82
4	Enhancing photocatalytic activity on gas-phase heavy metal oxidation with self-assembled BiOI/BiOCl microflowers. Journal of Colloid and Interface Science, 2019, 546, 32-42.	9.4	73
5	Spherical-shaped CuS modified carbon nitride nanosheet for efficient capture of elemental mercury from flue gas at low temperature. Journal of Hazardous Materials, 2021, 415, 125692.	12.4	64
6	Constructing 2D BiOIO3/MoS2 Z-scheme heterojunction wrapped by C500 as charge carriers transfer channel: Enhanced photocatalytic activity on gas-phase heavy metal oxidation. Journal of Colloid and Interface Science, 2020, 562, 429-443.	9.4	62
7	A review of sorbents for high-temperature hydrogen sulfide removal from hot coal gas. Environmental Chemistry Letters, 2019, 17, 259-276.	16.2	53
8	Elemental Mercury Capture from Simulated Flue Gas by Graphite-Phase Carbon Nitride. Energy & Fuels, 2020, 34, 6851-6861.	5.1	51
9	Elemental Mercury Removal by MnO ₂ Nanoparticle-Decorated Carbon Nitride Nanosheet. Energy & Fuels, 2019, 33, 3089-3097.	5.1	50
10	Sorbents for hydrogen sulfide capture from biogas at low temperature: a review. Environmental Chemistry Letters, 2020, 18, 113-128.	16.2	49
11	Nanosized ZnIn2S4 supported on facet-engineered CeO2 nanorods for efficient gaseous elemental mercury immobilization. Journal of Hazardous Materials, 2021, 419, 126436.	12.4	49
12	Photocatalytic oxidation removal of elemental mercury from flue gas.ÂA review. Environmental Chemistry Letters, 2020, 18, 417-431.	16.2	40
13	Co3O4/g-C3N4 Hybrids for Gas-Phase HgO Removal at Low Temperature. Processes, 2019, 7, 279.	2.8	38
14	CeO2-La2O3/ZSM-5 sorbents for high-temperature H2S removal. Korean Journal of Chemical Engineering, 2016, 33, 1837-1845.	2.7	35
15	CuO/g-C3N4 nanocomposite for elemental mercury capture at low temperature. Journal of Nanoparticle Research, 2018, 20, 1.	1.9	33
16	Perovskite LaMnO3/ZSM-5 composites for H2S reactive adsorption at high temperature. Adsorption, 2016, 22, 327-334.	3.0	29
17	Cu Nanoparticles Inlaid Mesoporous Carbon Aerogels as a High Performance Desulfurizer. Environmental Science & Technology, 2016, 50, 5370-5378.	10.0	27
18	Fabrication of Z-Scheme Heterojunction g-C ₃ N ₄ /Yb ³⁺ -Bi ₅ O ₇ I Photocatalysts with Enhanced Photocatalytic Performance under Visible Irradiation for Hg ^O Removal. Energy & Fuels, 2020, 34, 16445-16455.	5.1	26

Å>1⁄2Ç | 1 Ä3⁄4¯

#	Article	IF	CITATIONS
19	Elemental mercury captureÂfrom industrial gas emissions using sulfides and selenides: a review. Environmental Chemistry Letters, 2021, 19, 1395-1411.	16.2	26
20	A tin-based perovskite solar cell with an inverted hole-free transport layer to achieve high energy conversion efficiency by SCAPS device simulation. Optical and Quantum Electronics, 2021, 53, 1.	3.3	25
21	Effect of flue gas on elemental mercury removal capacity of defective carbonaceous surface: A first-principles study. Journal of Hazardous Materials, 2021, 404, 124013.	12.4	23
22	CuOâ€CeO ₂ /ZSMâ€5 composites for reactive adsorption of hydrogen sulphide at high temperature. Canadian Journal of Chemical Engineering, 2016, 94, 2276-2281.	1.7	22
23	Fabrication of Carbon-Modified BiOI/BiOIO3 Heterostructures With Oxygen Vacancies for Enhancing Photocatalytic Activity. Catalysis Letters, 2018, 148, 3349-3362.	2.6	21
24	One-Pot Synthesized BiOI/TiO2 Heterostructure with Enhanced Photocatalytic Performance and Photocatalytic Treatment of Gas-Phase Hg0. Catalysis Letters, 2018, 148, 2337-2347.	2.6	21
25	Enhanced photocatalytic activity of TiO2/graphene by tailoring oxidation degrees of graphene oxide for gaseous mercury removal. Korean Journal of Chemical Engineering, 2019, 36, 115-125.	2.7	21
26	Copper Sulfide-Loaded Boron Nitride Nanosheets for Elemental Mercury Removal from Simulated Flue Gas. Energy & Fuels, 2021, 35, 2234-2242.	5.1	19
27	Fabrication of a Z-Scheme Heterojunction Polyhedral-Shaped BiOIO ₃ /MIL-53(Fe) Photocatalyst for Enhancing Gaseous Hg ⁰ Removal. Energy & Fuels, 2021, 35, 3252-3265.	5.1	19
28	Molten salt synthesis of WS2 and MoS2 nanosheets toward efficient gaseous elemental mercury capture. Science of the Total Environment, 2022, 824, 153934.	8.0	19
29	Fabrication of BiVO4/BiOIO3 Heterojunctions via Hydrothermal Method for Photocatalytic Activity Under Visible Light. Catalysis Letters, 2018, 148, 3193-3204.	2.6	18
30	Study on Low-Temperature SCR Denitration Mechanisms of Manganese-Based Catalysts with Different Carriers. Water, Air, and Soil Pollution, 2020, 231, 1.	2.4	18
31	Preparation of CeO ₂ /CaO with Anti-sintering for Efficient Capture of As ₂ O ₃ from Flue Gas at a High Temperature. Energy & Fuels, 2021, 35, 20197-20205.	5.1	18
32	Study of Sheetlike BiOI/Rodlike Bi ₅ O ₇ I Composite Photocatalyst by In Situ Crystallization of BiOI with pH-Dependence for Hg ⁰ Removal. Energy & Fuels, 2021, 35, 11415-11426.	5.1	17
33	Microscopic Spherical α-Fe ₂ O ₃ for Highly Efficient Gaseous Arsenic Capture in Simulated Flue Gas Under a Wide Temperature Range. Energy & Fuels, 2021, 35, 19581-19591.	5.1	16
34	Nanosized Zn-In spinel-type sulfides loaded on facet-oriented CeO2 nanorods heterostructures as Z-scheme photocatalysts for efficient elemental mercury removal. Science of the Total Environment, 2022, 813, 151865.	8.0	16
35	Salt-Assisted Synthesis of Rod-Like Bi ₂ S ₃ Single Crystals for Gas-Phase Elemental Mercury Removal. Energy & Fuels, 2022, 36, 2591-2599.	5.1	15
36	Graphitic Carbon Nitride for Gaseous Mercury Emission Control: A Review. Energy & Fuels, 2022, 36, 4297-4313.	5.1	15

Å>1⁄2Ç | 1 Ä3⁄4⁻

#	Article	IF	CITATIONS
37	Gaseous Elemental Mercury Capture by Magnetic FeS ₂ Nanorods Synthesized via a Molten Salt Method. ACS Applied Nano Materials, 2022, 5, 2626-2635.	5.0	14
38	Experimental Study on the Influence of Surface Characteristics of Activated Carbon on Mercury Removal in Flue Gas. Energy & Fuels, 2020, 34, 6168-6177.	5.1	13
39	CuS-Doped Ti ₃ C ₂ MXene Nanosheets for Highly Efficient Adsorption of Elemental Mercury in Flue Gas. Energy & Fuels, 2022, 36, 2503-2514.	5.1	13
40	Nitrogen-rich biomass derived three-dimensional porous structure captures FeNi metal nanospheres: An effective electrocatalyst for oxygen evolution reaction. International Journal of Hydrogen Energy, 2022, 47, 12487-12499.	7.1	10
41	Investigation of CaO Influences on Fast Gasification Characteristics of Biomass in a Fixed-bed Reactor. Waste and Biomass Valorization, 2020, 11, 3731-3738.	3.4	8
42	HONEYCOMB-LIKE MESOPOROUS g-C ₃ N ₄ FOR ELEMENTAL MERCURY REMOVAL FROM SIMULATED FLUE GAS. Surface Review and Letters, 2020, 27, 2050017.	1.1	8
43	KINETIC BEHAVIOR OF ELEMENTAL MERCURY SORPTION ON CERIUM- AND LANTHANUM-BASED COMPOSITE OXIDES. Surface Review and Letters, 2019, 26, 1850141.	1.1	7
44	3D/0D Cu ₃ SnS ₄ /CeO ₂ Heterojunction Photocatalyst with Dual Redox Pairs Synergistically Promotes the Photocatalytic Reduction of CO ₂ . Energy & Fuels, 2022, 36, 7763-7774.	5.1	7
45	Elemental Mercury Adsorption by Cupric Chloride-Modified Mesoporous Carbon Aerogel. Colloids and Interfaces, 2018, 2, 66.	2.1	6
46	Rod-Shaped Bi ₂ S ₃ Supported on Flaky Carbon Nitride for Effective Removal of Elemental Mercury in Flue Gas. Energy & Fuels, 2021, 35, 14634-14646.	5.1	6
47	Improving the performance of organic lead–tin laminated perovskite solar cells from the perspective of device simulation. Optical and Quantum Electronics, 2022, 54, 1.	3.3	6
48	Improved NO removal from flue gas by hydrazine and its mechanism analysis. Journal of Chemical Technology and Biotechnology, 2019, 94, 3263-3268.	3.2	5
49	Experimental study on cogasification mechanisms of straw and kitchen waste in the fixedâ€bed gasifier. International Journal of Energy Research, 2020, 44, 8578-8590.	4.5	5
50	Molybdenum trioxide impregnated carbon aerogel for gaseous elemental mercury removal. Korean Journal of Chemical Engineering, 2020, 37, 641-651.	2.7	5
51	Study on arsenic, selenium, and lead produced in coal combustion: bibliometric method. Environmental Science and Pollution Research, 2021, 28, 32190-32199.	5.3	5
52	First principles study on electronic properties and oxygen evolution mechanism of 2D bimetallic N-doped graphene. Journal of Molecular Graphics and Modelling, 2022, 111, 108101.	2.4	5
53	Oxidative desulfurization of fuel oil catalyzed by a carbon nitride supported phosphotungstic acid based dicationic ionic liquid. Reaction Chemistry and Engineering, 2022, 7, 1380-1390.	3.7	5
54	The preparation of slow-release fertilizers with biomass ash and water/waste acid solutions from desulfurization and denitrification of flue gas. Environmental Science and Pollution Research, 2022, , 1.	5.3	2

Å>¹/2Ç | ¹ Ä³/4⁻

#	Article	IF	CITATIONS
55	Fabrication and Fractality of Fe2O3-CeO2/ZSM-5 Composites for High-Temperature Desulfurization. Colloids and Interfaces, 2017, 1, 10.	2.1	1
56	Characterization and Reuse Investigation on Scrapped V2O5–WO3/TiO2 Catalysts Operated in Various Industrial Flue Gases for NH3-SCR Reactions. Waste and Biomass Valorization, 2021, 12, 2597-2608.	3.4	1
57	One new channel for the reduction of NO during gasification condition: An insight from DFT calculations. Combustion Science and Technology, 2023, 195, 2191-2209.	2.3	1
58	Research on the preparations and properties of fertilizer recycling from biomass ash, slags, and waste acid liquid from desulfurization and denitrification process of flue gas. Biomass Conversion and Biorefinery, 2024, 14, 3235-3247.	4.6	0
59	Effect of coloured TiO ₂ with different oxygen vacancy concentrations on the photocatalytic oxidation of gaseous mercury. International Journal of Environmental Analytical Chemistry, 0, , 1-10.	3.3	0